UNIVERSITY COLLEGE LONDON

MENG MECHANICAL ENGINEERING

MECH0074 ENGINEERING IN EXTREME ENVIRONMENTS

EXTREME PRESSURE COURSEWORK

Author:
Hasha Dar

Module coordinator:
Prof. Ian Eames

December 16, 2022

Contents

List of Figures

List of Tables

Part I

Review of expansion loops in the energy sector

1 Industrial applications of expansion loops

Thermal expansion and contraction is an everpresent issue for all piping systems. Thermal expansion is a natural phenomenon, linked with the kinetic energy of the moleculues. As the kinetic energy of moleculus increases, the intermolecular distance also increases. At macroscopic scales, this manifests as a potentially significant change in the shape, size, density, and volume of an object. Within the scope of a piping system, a change in temperature of a pipe fixed with supports is problematic because the change in shape will result in induced stress. Over time, these stresses may fatigue the piping system, causing leaks. A pipe may change temperature due to environmental effects (day-night cycle, sun shining on a pipe) or due to the working fluid working within the pipe (superheated steam, liquid nitrogen). Hence, building piping systems with the ability to combat this thermal expansion is important to protect the system.

A few solutions exist to combat thermal expansion. One such example is the expansion loop. Figure 1 shows an expansion loop in a 2D and 3D configuration. The expansion loop acts to absorb the thermal expansion from the adjacent piping. The size and location of an expansion loop is primarily determined through code - for piping this is ASME B31.8. Before we can start designing a system, some requirements of the system must be first understood. Typically, one will know the working fluid of the system and hence can determine the temperature changes within the system. One will also most likely know where the working fluid is to go with flow rate requirements. This will determine the size and material of piping in the system. Equation (1) shows how thermal expansion or contraction can be calculated for a given material.

$$\Delta L = \alpha L_{pipe} \Delta T \tag{1}$$

where ΔL is the change in length, α is the coefficient of thermal expansion of the material, L_{pipe} is the length of the pipe and ΔT is the change in temperature. Different materials will have different thermal properties and hence will expand or contract at different rates. However, these materials will also have different mechanical properties such as higher (or lower) working stress or modulus of elasticity. The pipe's thickness and outer diameter will also determine the maximum stress of the pipe. Figure 2 shows the rate at which different materials change length with temperature. It can be seen that plastic based materials expand much more quickly than metals in general.

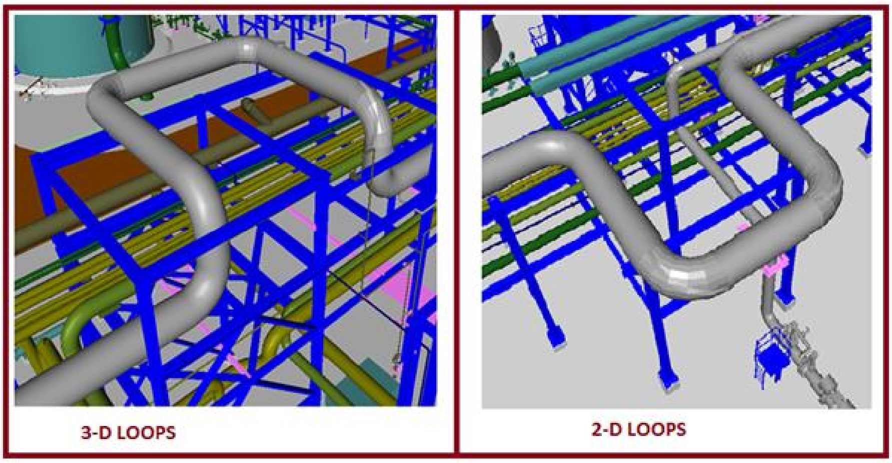

Figure 1: Expansion loops shown in a 2D and 3D configuration [1].

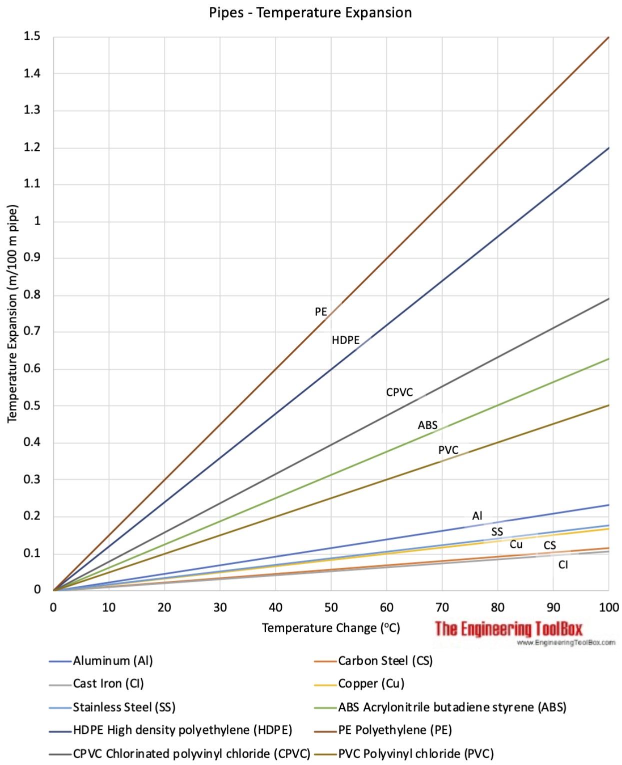

Figure 2: Thermal expansion for different materials [2].

Bibliography

[1] Anup. Kumar Dey. Expansion loops on the piping or pipeline systems. https://whatispiping.com/expansion-loop-on-piping-system/ [Accessed: 16-12-22], 2019.

[2] Engineering ToolBox. Piping materials - temperature expansion coefficients. [online]. https://www.engineeringtoolbox.com/pipes-temperature-expansion-coefficients-d_48.html [Accessed: 16-12-22], 2003.

Part II

Technical assessment of water hammer for expansion loops

2 Frequency of the water hammer pressure fluctuation in a pipe

2.1 MATLAB script

2.1.1 Pressure fluctuation and Joukowski prediction

The calculation for maximum magnitude of the water hammer pulse is (2). This is also known as the Joukowski equation.

$$\Delta p = \rho a_0 \Delta v \, (\text{Pa}) \tag{2}$$

where Δp is the change in pressure, ρ is the fluid density, a_0 is the sonic velocity in the pipe and Δv is the change in fluid velocity. Running the MATLAB script with the values shown in Table 1, Figure 3 was generated.

The pressure values at the first peak of the rise were chosen to find the maximum pressure differential. A settled pressure differential value was also found (shown in Figure 4). Table 2 shows the maximum pressure differentials for each index point (s- value: point along length of pipe from valve) and the pressure differential of the settled value.

The Joukowski prediction makes assumptions in order to calculate a value for our pressure differential. This may explain the discrepancy we see for our differential values. For example, the Joukowski prediction does not account for frictional losses within the system. We also assume there is no column separation, cavitation or any other fluid effects.

Parameter	Value
a_0	$1100\,\text{m}\,\text{s}^{-1}$
ρ	$455\,\text{kg}\,\text{m}^{-3}$
Δv	$1.5\,\text{m}\,\text{s}^{-1}$
$\Delta p_{joukowski}$	$750\,750\,\text{Pa}$

Table 1: Values for Joukowski Prediction and calculated pressure differential.

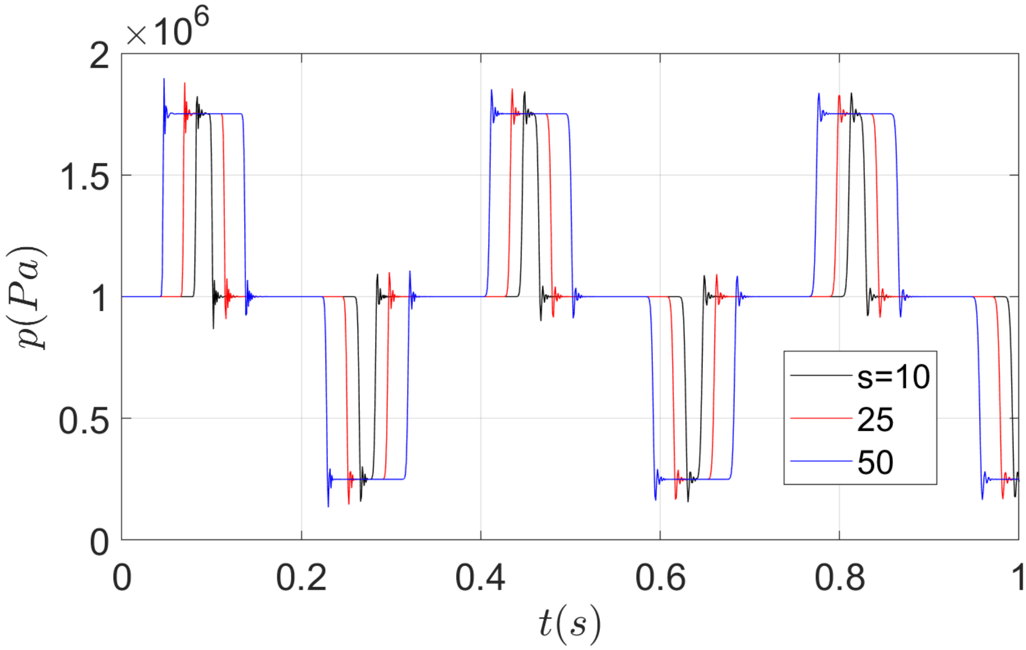

Figure 3: MATLAB script results showing pressure against time for $s = 10,\ 25,\ 50$ m.

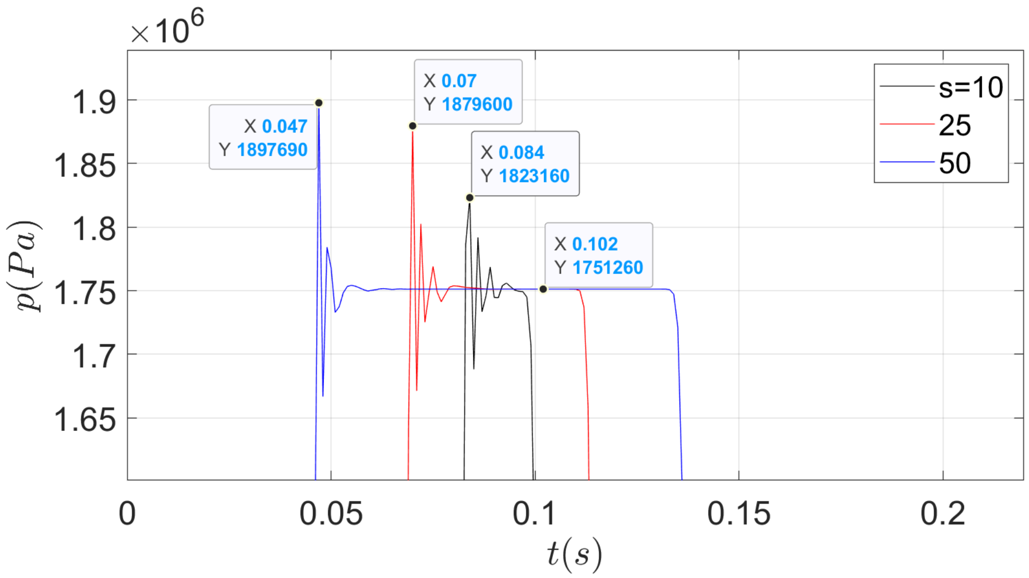

Figure 4: Index points for finding maximum pressure differential and settled pressure differential.

s- **value**	**Maximum pressure differential**/Pa	**Percentage difference compared to analytical**
10	823160	8.80%
25	879600	14.65%
50	897690	16.37%
Settled value	751260	0.08%

Table 2: Pressure differentials for indexed s- values and settled values.

2.1.2 Frequencies associated with pressure fluctiation and analytical prediction

An analytical result for the frequencies of the pressure fluctuation can be found using (3)[1].

$$T = \frac{1}{f} = \frac{2L}{c} = \frac{2 \cdot s}{1100} \tag{3}$$

Indexing the values found in our MATLAB result, we can find the frequencies of the pressure fluctuation in Table 3. The index points were selected as the first peak of the rise and the first peak of the return to $1\,\mathrm{MPa}$. The time between these points represents the duration of the pressure rise from the wave propagating past a particular point in the pipe. The results show a relatively low percentage error. Our discrepancy may stem from a lack of temporal resolution, as we are only using a time step of $1 \times 10^{-3}\,\mathrm{s}$. A higher time-step may allow us to accurately find the value of the first peaks.

s- value	**Frequency**/Hz		**Percentage**
	MATLAB	**Analytical**	**difference**
10	10.99	11	0.09%
25	21.74	22	1.18%
50	55.56	55	1.02%

Table 3: Frequency of pressure fluctuation.

2.2 Force analysis

Using MATLAB, the forces acting on each bend of the loop were calculated. Figure 5 shows the magnitude of the force acting on each bend for the given time period. This was calculated by taking the component forces in each direction and using (4) to calculate the magnitude. The force orientations are specific to the problem and it is assumed that the total force applied from the pressure wave can be averaged over the entire bend i.e. assumed as a single concentrated force acting normal to the centre of the bend. For the purposes of calculation, the positive x-axis was taken as $0°$ with counter-clockwise taken as positive.

$$F = \sqrt{F_x^2 + F_y^2} \tag{4}$$

Figure 6 shows a plot of the forces from the first reflection of the pressure wave. We see that the waves are reflected multiple times through the expansion loop, decreasing in magnitude on each reflection. For the purposes of finding the force exterted on the bend due to the reflection of the pressure wave, the peak forces from the first reflection were chosen. Figure 7 shows the direction of the force acting on each bend. Table 4 shows the magnitude and direction of the force acting at each bend, and the overall force exerted on the expansion loop. We find that the expansion loop experience a net force pushing it to the left with a slight downwards push.

[1] Referenced from ‘Piping Handbook Seventh Edition’ by Mohinder L. Nayyar, page 1266, publisher: McGraw-Hill

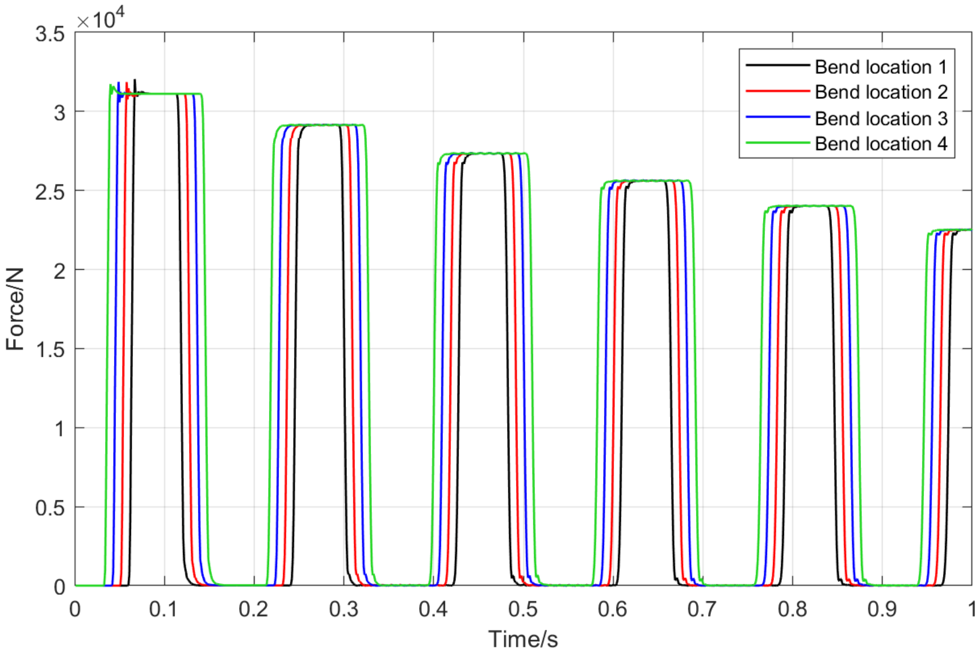

Figure 5: Magnitude of force on each bend from reflections of pressure wave over the time period.

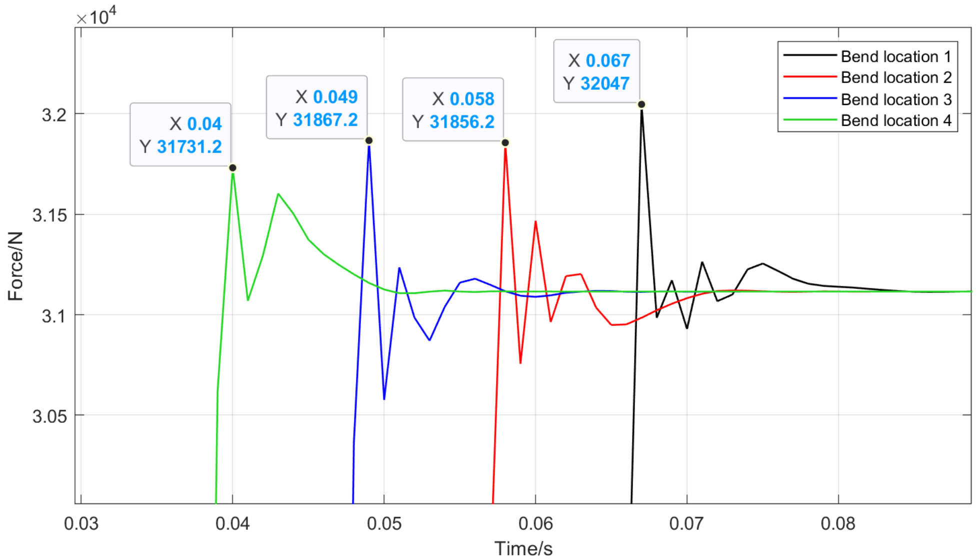

Figure 6: Forces on each bend from first reflection of pressure wave.

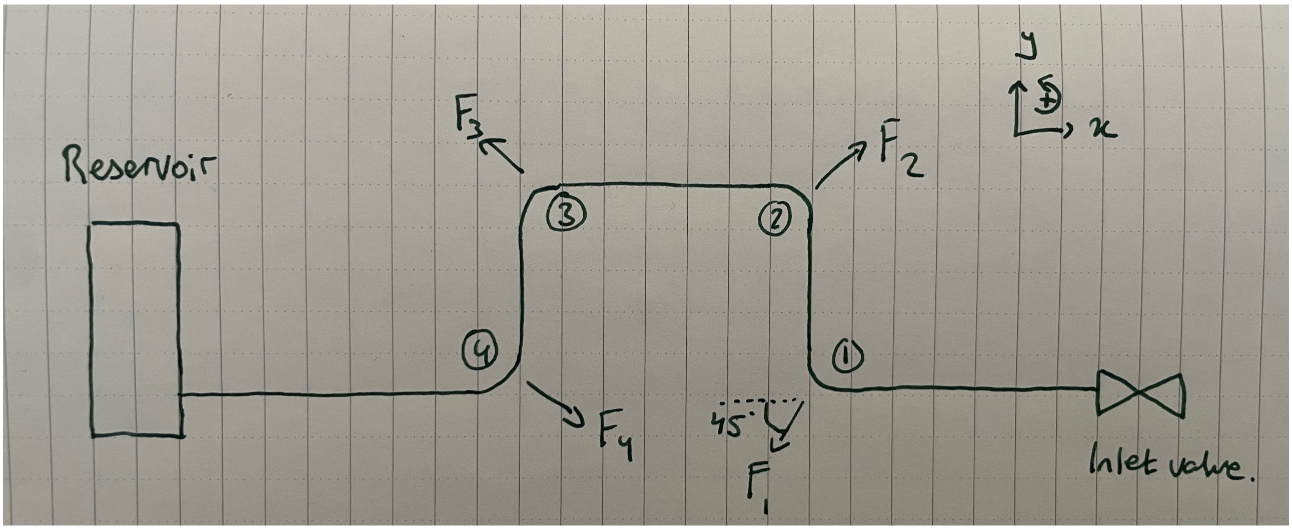

Figure 7: Schematic showing forces acting on expansion loop.

Bend location	**Magnitude of force**/N	**Direction**/degrees
1 ($s = 35$ m)	32047	225
2 ($s = 45$ m)	31856	45
3 ($s = 55$ m)	31867	135
4 ($s = 65$ m)	31731	315

Table 4: Table to show magnitude and direction of forces acting on the expansion loop.

The total force on the entire expansion loop was found to be:

$$F_{total,x} = -231.2\,\text{N} \tag{5}$$

$$F_{total,y} = -38.9\,\text{N} \tag{6}$$

$$F_{total} = 234.4\,\text{N} \tag{7}$$

$$F_{orientation} = 9.55^{\circ} \tag{8}$$

3 Modal analysis of expansion loop

3.1 Modal analysis of a cantilevered pipe

In order to conduct our ANSYS analysis, we need to find the effective pipe density, we can use (9).

$$\rho_{eff} = \rho_s + \rho_{LNG}\left(\frac{d_i^2}{d_e^2 - d_i^2}\right) \tag{9}$$

Table 5 shows the values used in the ANSYS simulations.

Parameter	Value
d_i	793.94 mm
d_e	813 mm
ρ_s	7850 kg m^{-3}
ρ_{LNG}	455 kg m^{-3}
ρ_{eff}	$17\,214.06$ kg m^{-3}

Table 5: Values for cantilevered beam analysis in ANSYS.

3.1.1 List of unique frequencies & mesh sensitivity test

Table 6 shows values of the modal frequencies for a cantilevered pipe with lengths $L = 10,\ 20,\ 30$ m. For the theoretical values, we can calculate the bending moment of a cantilevered beam using (10).

$$f_n = \frac{\alpha_n^2}{2\pi}\left(\frac{EI}{AL^4}\right)^{\frac{1}{2}} \tag{10}$$

$$I = \frac{A}{16}\left(d_e^2 + d_i^2\right) \tag{11}$$

where coefficient α_n values were found in literature. The theoretical values were calculated using MATLAB (Appendix A.2)

Mode	Frequency/Hz					
	ANSYS	Theory	ANSYS	Theory	ANSYS	Theory
	$L = 4$ m		$L = 10$ m		$L = 20$ m	
1	31.65	33.86	5.35	5.42	1.35	1.35
2	149.93	212.23	31.49	33.96	8.37	8.49
3	332.21	594.32	80.99	95.09	22.69	23.77
4	521.06	1164.66	143.54	186.35	42.93	46.59
5	712.09	1925.06	214.08	308.01	68.06	77.00
6	857.22	2875.85	289.12	460.14	97.07	115.03

Table 6: Table to show values of modal frequencies for a cantilever beam of length $L = 10,\ 20,\ 30$ m, compared to theoretical values.

A mesh sensitivity test was conducted using the $L = 4$ m case. The element size was varied from 0.5 m to 0.01 m and the modal frequencies were found. By taking the frequency of a particular mode and element size and comparing it to the frequency found in the simulation with element size 0.01 m (for the same mode), a percentage difference was calculated. Figure 8 shows how frequency values converge. We see that the percentage difference in frequency for element size 0.125 m and smaller is negligible. Hence, for the simulations conducted, a mesh size of 0.125 m was used.

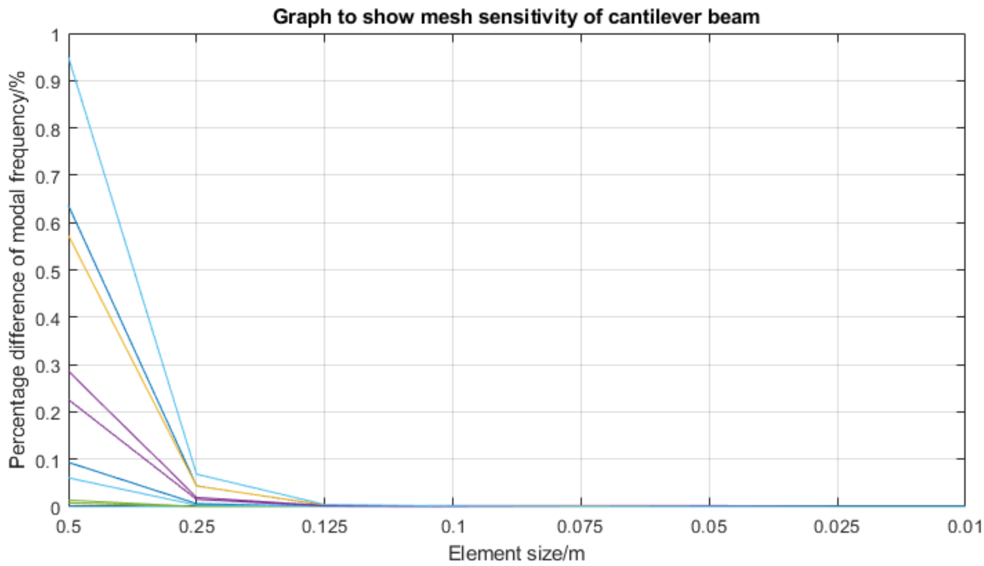

Figure 8: Mesh sensitivity test results. Conducted on a beam with length $L = 4\,\text{m}$.

3.1.2 Differences and similarities between theoretical and calculated modes

Using MATLAB, the percentage difference between the ANSYS values and the theoeretical values was found. This is shown in Table 7.

Mode	Percentage difference (%)		
	$L = 4\,\text{m}$	$L = 10\,\text{m}$	$L = 20\,\text{m}$
1	7.00	1.27	0.34
2	41.56	7.84	1.43
3	78.90	17.41	4.77
4	123.52	29.82	8.52
5	170.33	43.88	13.14
6	235.49	59.15	18.51

Table 7: Table to show percentage difference between ANSYS modal frequencies and theoretical values.

We find that for lower L- values the modal frequencies are higher in our ANSYS simulation. This trend matches with the theoretical values, where modal frequency decreases as a function of L. For the first mode, we find that ANSYS and theory values are closely matched with single digit or decimal percentage difference. For higher modes, the percentage difference increases substantially. As L increases, our percentage difference between ANSYS and theoretical values decreases. As the mode number increases, the percentage difference increases.

As we are using the Euler-Bernoulli theorem to calculate our theory values, the assumptions made can potentially explain the discrepancy between our modal frequency values. One such assumption is that plane sections remain plane. We know that for higher modes, the beam undergoes a larger displacement, as more sections of the beam are displaced from the normal axis. This large displacement results in plane sections no longer remaining plane, making our assumption invalid for higher modes.

3.2 Modal analysis of an expansion loop

The geometry was constructed within ANSYS as shown in Figure 9. A circular tube profile was used and its geometry is shown in Figure 10. A number of constraints were applied to the geometry and are shown in Figure 11. At the ends of the pipe, we use fixed supports as we are investigating the modal frequencies of this specific section. For the lateral constraints, the justification for such a support is that the piping section should be allowed to slide back and forth within the support. This is because the pipe will thermally expand and contract under normal operation. Hence, this sliding motion will reduce the stress on the piping section, reducing cyclic fatigue. This lateral constraint also allows the pipe some degree of movement in the case of a water hammer, where if it was fixed laterally, may excessively wear (or even) damage the joint. A basic mesh sensitivity test was completed and the results are shown in Figure 12. A mesh size of 0.01 m was chosen as the percentage error is mostly converged and negligible.

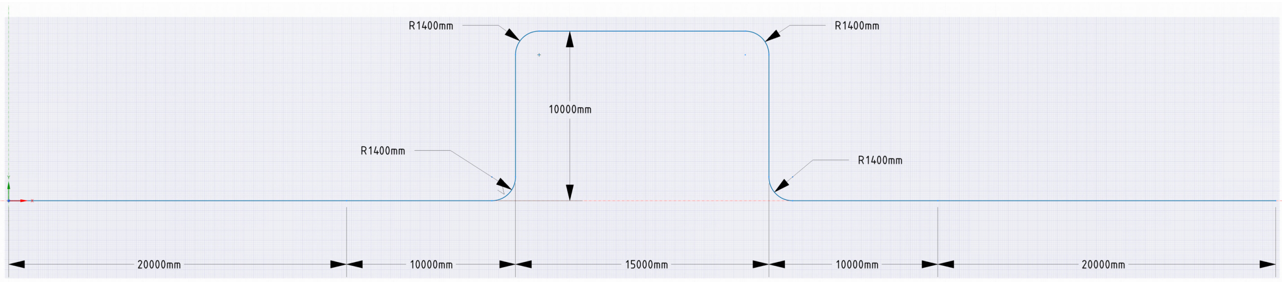

Figure 9: Geometry used for expansion loop modal analysis.

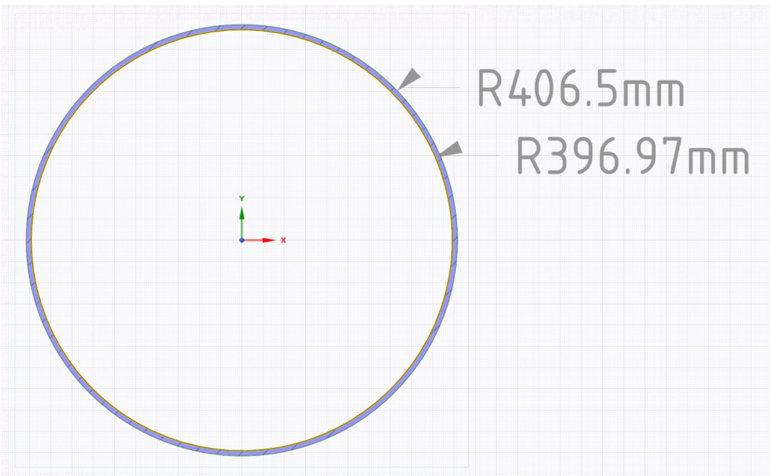

Figure 10: Geometry used for circular tube profile.

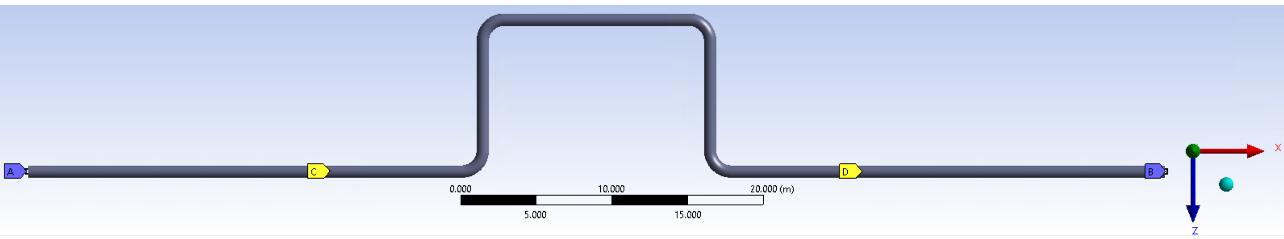

Figure 11: Constraints used for geometry. A & B: fixed constraints. C & D: y- and z- dimensions fixed, x-dimension free.

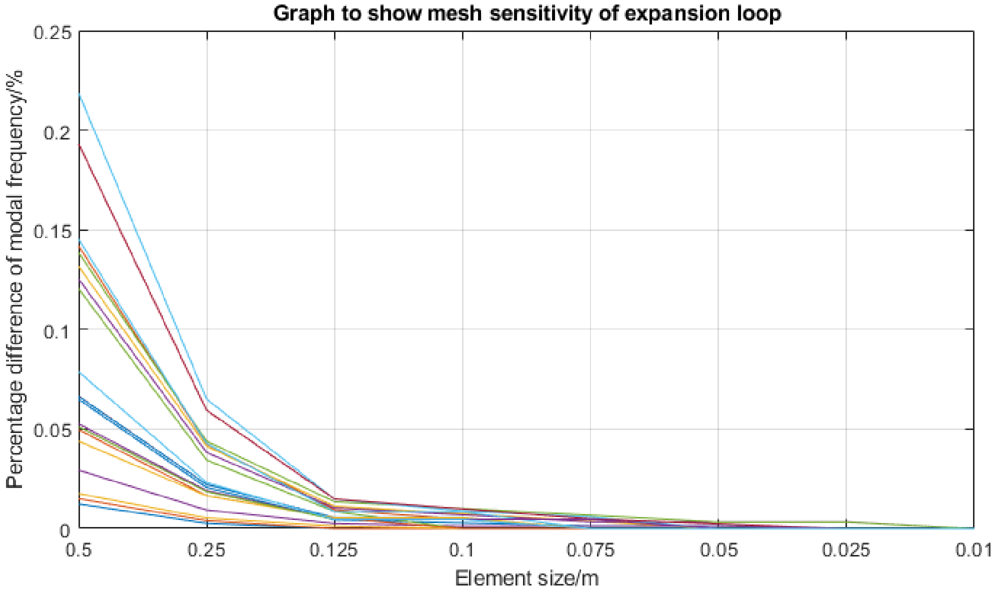

Figure 12: Mesh sensitivity test results for expansion loop.

The results from the simulation are shown in the following figures.

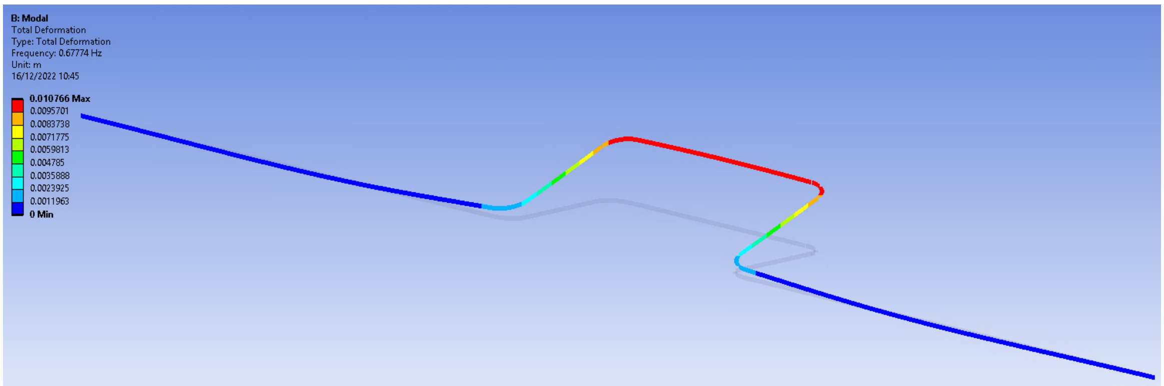

Figure 13: Modal frequency: $0.68\,\mathrm{Hz}$. Out-of-plane deformation.

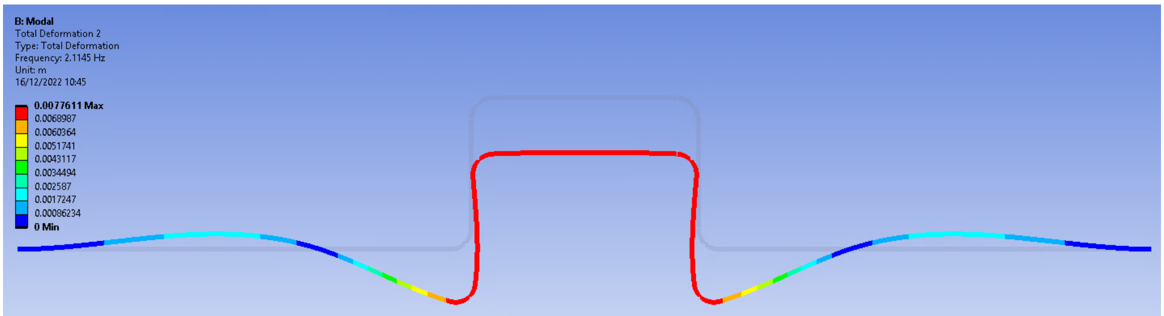

Figure 14: Modal frequency: $2.11\,\mathrm{Hz}$. In-plane deformation.

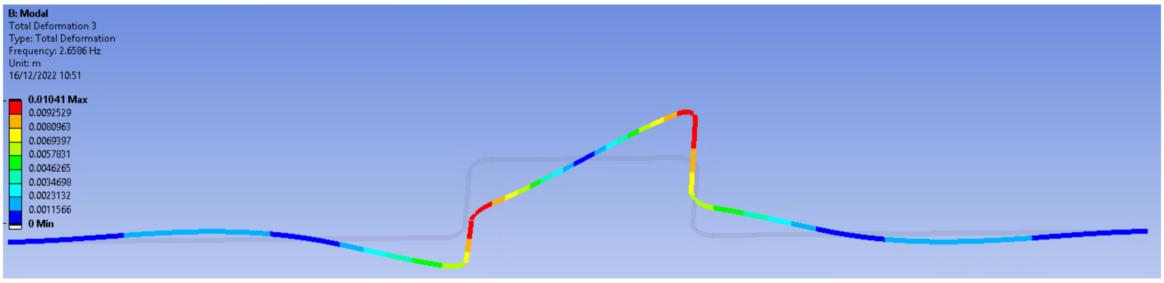

Figure 15: Modal frequency: 2.66 Hz. Out-of-plane deformation.

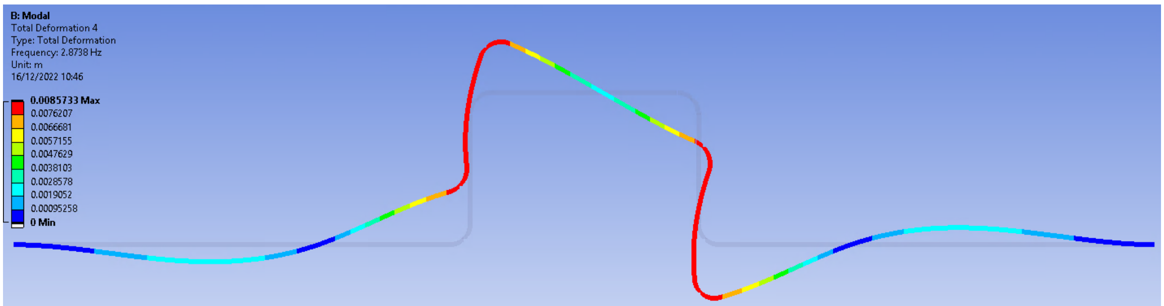

Figure 16: Modal frequency: 2.87 Hz. In-plane deformation.

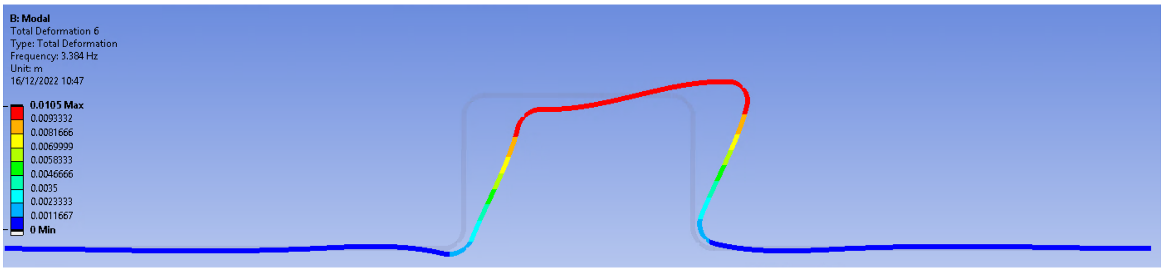

Figure 17: Modal frequency: 3.38 Hz. In-plane deformation.

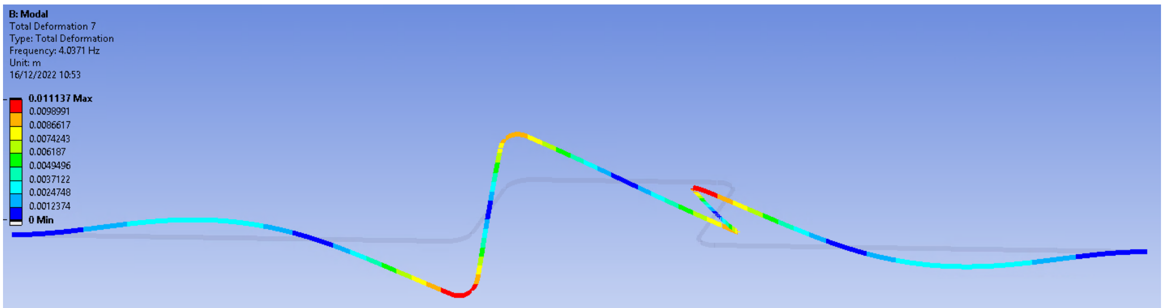

Figure 18: Modal frequency: 4.04 Hz. Out-of-plane deformation.

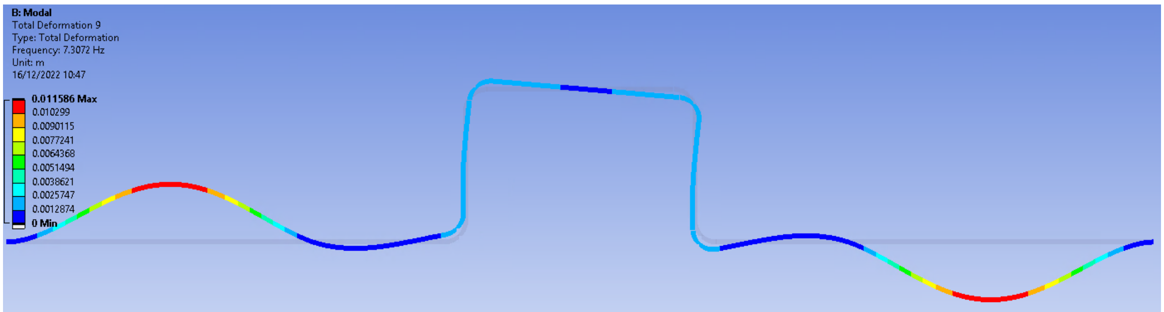

Figure 19: Modal frequency: $7.31\,\mathrm{Hz}$. In-plane deformation.

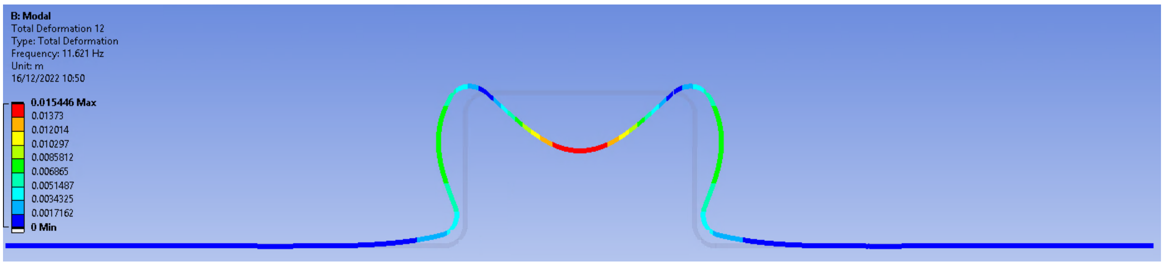

Figure 20: Modal frequency: $11.62\,\mathrm{Hz}$. In-plane deformation.

Figure 13 shows the loop section bending backwards and forwards out-of-plane. Figure 14 shows the loop bending upwards and downwards in-plane. Figure 15 shows the loop section twisting out-of-plane. Figure 16 shows the expansion loop twisting in-plane. Figure 17 shows the top section of the loop oscillating horizontally leftwards and rightwards. Figure 18 also shows a twisting motion within the loop section at a higher frequency (mroe sections of the loop are twisting). Figure 19 shows just the straight sections of the expansion loop oscillating in-plane. Figure 20 shows just the expansion loop oscillating in-plane at a higher mode frequency.

A MATLAB code

A.1 Mesh sensitivity plots

```
%HD

clc
clear
close all

%import data
data = readmatrix('data.xlsx','Sheet','L4','Range','A4:P23');
elSize = [0.5;0.25;0.125;0.1;0.075;0.05;0.025;0.01];

%array initialise
A = zeros(numel(data(:,1)),numel(data(1,:))/2);

%calculate percentage difference of result compared to 0.01m el size
for i = 1:8
   for j = 1:numel(data(:,1))
      A(j,i) = 100*(data(j,i*2) - data(j,end))/data(j,end);
   end
end

%plot
for i = 1:numel(A(:,1))
   plot(A(i,:))
   hold on
end
xticklabels(elSize);
grid on
axis auto
xlabel('Element size/m');
ylabel('Percentage difference of modal frequency/%');
title('Graph to show mesh sensitivity of cantilever beam')
hold off
```

A.2 Theoretical modal frequency values for cantilevered beam

```
%HD

clc
clear
close all

alpha = [1.875;4.694;7.855;10.996;14.137;17.279]; %modal bending coeffs
E = 200e9; %Youngs modulus GPa
L = [4;10;20]; %length of beams
de = 0.813; %external diameter m
di = 0.79394; %internal diameter m
rhoS = 7850; %density steel
rhoLNG = 455; %density gas
```

```
rhoEff = rhoS + rhoLNG*((di^2)/(de^2-di^2)); %density effective
A = (pi*(de/2)^2) - (pi*(di/2)^2); %cross-sectional area m^2
I = (A/16)*(de^2 + di^2); %second moment of inertia m^4

fn = zeros(3,6);
for i = 1:3
   for j= 1:6
      fn(i,j) =
         ((alpha(j)^2)/(2*pi))*((E*I)/(rhoEff*A*((L(i))^4)))^(0.5);
   end
end

fn = fn';

%import data
L4 = [31.65;149.93;332.21;521.06;712.09;857.22];
L10 = [5.35;31.49;80.99;143.54;214.08;289.12];
L20 = [1.35;8.37;22.69;42.93;68.06;97.07];

ANSYSFreqs = cat(1,L4',L10',L20')';

percDiff = zeros(numel(ANSYSFreqs(:,1)),numel(ANSYSFreqs(1,:)));

%percentage differences
for i = 1:numel(ANSYSFreqs)
   percDiff(i) = 100*(fn(i) - ANSYSFreqs(i))/ANSYSFreqs(i);
end
```